

Discovery of red-shifting mutations in firefly luciferase using high-throughput biochemistry

Clair M. Colee,^{1‡} Nicole M. Oberlag,^{1‡} Marcell Simon,^{1‡} Owen S. Chapman,² Lyndsey C. Flanagan,¹ Edison S. Reid-McLaughlin,¹ Jordan A. Gewing-Mullins,¹ Synaida Maiche,¹ Devi F. Patel,¹ Andre R.O. Cavalcanti,² and Aaron M. Leconte^{1}*

¹W.M. Keck Science Department of Claremont McKenna, Pitzer, and Scripps Colleges, Claremont, California, 91711, United States of America

²Department of Biology, Pomona College, Claremont, California, 91711, United States of America

Corresponding Author

*Telephone: 909-607-9353. Email: aleconte@kecksci.claremont.edu

Author Contributions

[‡]C.M.C., N.M.O., and M.S. contributed equally to this manuscript.

A.M.L. conceived the project; O.S.C. and A.R.O.C. performed statistical coupling analysis; L.C.F., E.R.M., and N.M.O. constructed the libraries; S.M., C.M.C., and N.M.O. performed screens; C.M.C., D.F.P., and M.S. performed characterization of mutants identified via screening; J.A.G-M. and A.M.L. developed code to analyze sequencing data; C.M.C., M.S., and A.M.L. performed data analysis; M.S., N.M.O., C.M.C., and A.M.L. wrote the manuscript with input from all authors. All authors have given approval to the final version of the manuscript.

Acknowledgements

This work was supported by the U.S. National Institutes of Health (1R15GM135860 award to A.M.L.). M.S. was supported by the Cottrell postbaccalaureate fellowship from the Research Corporation for Science Advancement (CS-PBP-2023-016). We thank Dylan McKuskey (of the Sheung laboratory of the Keck Science Department) for developing the script used for curve fitting. We also thank Prof. Jennifer Prescher and members of the Prescher laboratory for helpful discussions.

Notes

The authors declare no competing financial interests.

ABSTRACT

The *Photinus pyralis* luciferase (FLuc) has proven a valuable tool for bioluminescence imaging, but much of the light emitted from the native enzyme is absorbed by endogenous biomolecules. Thus, luciferases displaying red-shifted emission enable higher resolution during deep-tissue imaging. A robust model of how protein structure determines emission color would greatly aid the engineering of red-shifted mutants, but no consensus has been reached to date. In this work, we apply deep mutational scanning to systematically assess twenty functionally important amino acid positions on FLuc for red-shifting mutations, predicting that an unbiased approach would enable novel contributions to this debate. We report dozens of red-shifting mutations as a result, a large majority of which have not been previously identified. Further characterization revealed that mutations L286V and T352M, in particular, cause pure red emission with much of the light being >600 nm. The red-shifting mutations identified by this high-throughput approach provide strong biochemical evidence for the multiple-emitter mechanism of color determination, and point to the importance of a water network in the enzyme binding pocket for altering the emitter ratio. This work provides a broadly applicable mutational data set tying FLuc structure to emission color that informs our mechanistic understanding of emission color determination and should facilitate the further engineering of improved probes for deep-tissue imaging.

ABBREVIATIONS

| | |
|------------------|---|
| BLI | Bioluminescence imaging |
| D-luc | D-luciferin |
| FLuc | Firefly luciferase from <i>P. pyralis</i> |
| HT-Seq | High-throughput sequencing |
| SCA | Statistical coupling analysis |
| WT | Wild-type |
| λ_{\max} | Wavelength of maximum emission intensity |

INTRODUCTION

Luciferase enzymes catalyze a multi-step chemical reaction using a substrate, luciferin, that generates visible light as a byproduct. They are found in a diverse array of organisms, including fungi, fireflies, and an estimated 80% of deep sea eukaryotes.^{1,2} Different species possess varying luciferase and luciferin structures which, in turn, emit light of varying wavelengths.

Bioluminescence, defined as the emission of visible light from cells or organisms, is not only important in nature, but is also a powerful biomedical research tool for tracking a range of biological molecules, such as viruses and tumor cells, and biological events such as cell movement and enzymatic activity.^{3,4} The most commonly used reporter in bioluminescent imaging (BLI) is firefly luciferase from *Photinus pyralis* (FLuc); it is one of the most biostable luciferases, displays rapid turnover, and its cognate luciferin (D-luciferin) has high bioavailability.³ FLuc achieves bioluminescence by deploying Mg-ATP and molecular oxygen to oxidize D-luciferin, producing an excited oxyluciferin product that emits a photon of around 560 nm upon relaxation to the ground state.⁵ One limitation of wild-type FLuc for biomedical imaging applications is that the enzyme's natural emission peaks in the yellow-green range of the visible spectrum.⁴ During *in vivo* imaging, this light can be absorbed by the endogenous molecules such as hemoglobin, myoglobin, and melanin, which predominantly absorb all visible wavelengths except for red light.⁶ Thus, deep tissue imaging can be improved by red-shifting the wavelength of FLuc emission beyond 600 nm.⁶

Various protein engineering strategies have been applied to red-shift FLuc emission for this purpose. Other beetle luciferases homologous to FLuc, by oxidizing the same D-luciferin substrate, emit wavelengths ranging from 538 nm (*Amydetes vivianii*) to 628 nm (*Phrixothrix hirtus*).^{3,7} Introducing mutations conserved among red-shifted homologs to FLuc has enabled the red-shifting of its natural emission spectrum, but has simultaneously impaired protein stability, thus resulting in reduced photon output. Random mutagenesis and directed evolution of FLuc and homologous enzymes, meanwhile, have also yielded strongly red-shifted mutants including F247A, S284T, and E455K (*P. pyralis* numbering used throughout).^{8,9} However, these approaches also tend to yield reduced photon output. These prior studies also tend to yield a small number of mutant enzymes; thus, they have provided little biochemical information on the complex structural and mechanistic factors affecting emission wavelength.

For the efficient and even rational alteration of FLuc emission color, a robust model of the color tuning mechanism is needed. It is well established that D-luciferin as a luminophore is highly sensitive to its local environment; solvent studies,¹⁰ mutational evidence,^{9,11} and the existence of natural red- and blue-shifted homologs^{12,13} that process the same substrate have clearly demonstrated that the protein environment plays a key role in the emission wavelength. Despite significant research efforts, which have led to diverse theories regarding color determination, a conclusive model remains elusive. Some evidence suggests that the tautomeric and charge state of the oxyluciferin emitter, where each form displays a characteristic wavelength, determines the color.^{8,14} Other studies have found that various 'microenvironment' effects attributed to the enzyme, such as tightness of the binding pocket, hydrogen-bond networks, active site polarity, and local charge distribution alter the emission color as well.^{7,15} To further complicate matters, many residues that affect emission color are distributed all throughout the protein tertiary structure, and many mutations may support multiple hypotheses.⁷ Biochemical studies have often focused on a limited number of mutations in search of relevant interactions, while others have focused on the electronic properties of oxyluciferin with little regard for the enzyme's role. Unsurprisingly, these disparate approaches have led to conflicting conclusions about the relative contribution of each factor to emission wavelength, undermining any consensus on the overall mechanism.

As a novel approach to addressing this challenging question, we hypothesized that screening many amino acid positions with an unbiased and systematic approach may rapidly produce a large amount of biochemical information which, in turn, may help to elucidate the mechanism of color tuning. Modern innovations in DNA sequencing and molecular cloning have enabled the high-throughput discovery of novel mutations from large pools of mutant enzymes. For example, deep mutational scanning assigns function to many mutations in parallel with a single experiment by leveraging screening and selection methods combined with high-throughput sequencing (HT-Seq).¹⁶ Specifically, this approach enables the systematic assessment of every possible amino acid permutation at positions of interest, and thus the evaluation of many more mutants for functional changes than traditional hypothesis-based mutagenesis allows. This technique has enabled the discovery of impactful new mutations across multiple fields, from identifying thermodynamically stabilizing mutations for pharmaceutical purposes to hyperactive mutations in ubiquitin that provided biochemical insights.^{16,17} While deep mutational scanning is clearly effective in identifying novel mutations to shed new light on complex catalytic mechanisms, it has not yet been applied to luciferase to study the color tuning mechanism.

Here, we apply deep mutational scanning to twenty amino acid positions identified using a bioinformatic method, statistical coupling analysis (SCA). SCA identifies functionally important amino acids regardless of spatial location or their role in catalysis by identifying networks of functionally coupled amino acids.¹⁸ SCA has proven valuable in research on protein folding, structure, and allostery, as well as to identify minimal amino acid motifs for changing biochemical functions.^{19,20} Previously, we applied SCA to identify functionally important residues and surveyed a small number of mutations at those sites to find luciferases with increased thermostability and red-shifted emission.²¹ In this work, we systematically evaluate all 380 amino acid changes at 20 SCA-identified positions on FLuc for red-shifted emission properties. We report novel FLuc mutants with emission maxima above 600 nm, as well as a rich data set that ties hundreds of amino acid changes to protein activity and emission color. This study both informs our understanding of the mechanistic basis of color determination and provides a broadly applicable resource for both mechanistic biochemists and protein engineers.

RESULTS

SCA and library construction

While deep mutational scanning is a powerful method to evaluate all possible permutations, established luciferase screening methods make it operationally impractical to scan all or even much of the FLuc protein—even as single mutants. Thus, the choice of positions to mutate was an extremely important initial consideration. To prioritize protein residues likely to alter FLuc luminescence upon nonsynonymous mutation, we applied the SCA algorithm.¹⁸ Briefly, SCA performs feature extraction and clustering to identify residues that are hypothesized to share functional or evolutionary properties, termed ‘sectors’. We applied SCA to a multiple sequence alignment of 284 evolutionarily conserved luciferases and CoA ligases and identified 4 protein sectors of sizes 23, 37, 7 and 38 amino acid residues (**Table S1**). The sector of size 37 was significantly enriched for residues previously implicated in modulating the bioluminescence wavelength of firefly luciferases (χ^2 test, $p = 0.0004$, $q = 0.004$). Spatially, residues of this sector were tightly co-located at and adjacent to the catalytic site (**Figure S1**). Residues in this sector were significantly more likely to physically contact each other on the three-dimensional free FLuc structure (PDB: 5DV9) than random sets of equivalent size (permutation test, $p = 0.01$). We

therefore hypothesized that novel mutations to residues in this cluster would be likely to modulate FLuc function.

To systematically evaluate all possible mutations at the 20 SCA-identified positions that contribute most to the sector, we constructed individual libraries at each position by joining synthetic inserts containing degenerate NNK codons at the position of interest with a PCR-generated vector using Gibson assembly. Successful library construction was confirmed following cloning by sequencing, which confirmed that mutations had been introduced at the intended positions. Having created a diverse set of 20 libraries encoding 380 total nonsynonymous FLuc mutations, we were ready to comprehensively survey each library to glean biochemical insights and identify red-shifted enzymes.

Identification of active FLuc mutants

We developed and validated a high-throughput workflow to assess these mutations (**Figure 1**). Briefly, all libraries were first subjected to a primary screen which identified active mutants. Then, active mutants were subjected to a secondary screen for emission wavelength. To connect function changes to genotypes, mutants were collected to create enriched populations for specific functions and subjected to high-throughput DNA sequencing (HT-Seq), where initial data processing was aided by the EasyDIVER pipeline.²² Then, by comparing the abundance of mutations in different populations, we can assign likely function changes to specific mutations.

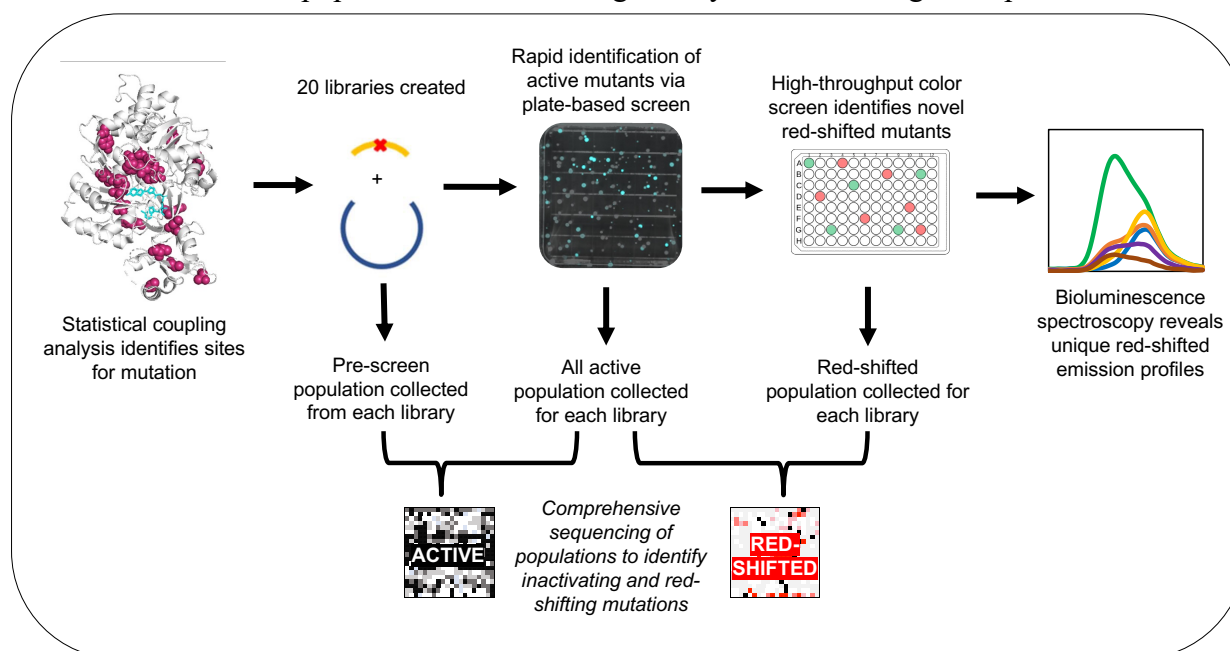


Figure 1. Scheme detailing our combination of bioinformatics-guided library design (selected positions show in magenta at left) with deep mutational scanning to identify novel red-shifting mutations.

First, to differentiate active mutants from inactive ones, we employed a previously developed top-plating method to screen all mutants for bioluminescent activity.²¹ Individual SCA libraries were embedded in a thin layer of top agar containing transformants, isopropyl β -D-thiogalactopyranoside (IPTG) to induce protein expression, and D-luciferin. Under these conditions, active mutants emit light, allowing for their identification using a CCD camera. For each individual library, at least 200 library members were assessed and active mutants were identified and collected into enriched populations. This essential initial step allows the efficient

separation of active from inactive members, facilitating screening for function changes downstream.

Beyond identifying individual active colonies, this general activity screen also revealed the percentage of active mutants in each library and, by extension, the relative mutability of each native amino acid (**Figure 2A**). To assess reproducibility of this mutability value, we re-screened ten libraries that spanned a range of activities, and found this method to be highly reproducible (**Figure S2**). Importantly, amino acid positions that are mutable, but that still contribute to function, are particularly valuable for engineering efforts.²³ Libraries containing the highest percentages of active colonies, such as I120X (65%), H431X (81%), and A477X (76%), suggest wild-type residues that are highly mutable. Conversely, amino acid positions that are highly immutable often reveal valuable information about protein mechanisms. Positions Y53 (8%), T191 (14%), and T346 (3%) were found to be largely immutable, implying an important functional role for these positions despite their varied distribution throughout the tertiary structure and, in some cases, significant distance from the active site of the protein. Thus, we have been able to assess mutability, a valuable piece of biochemical information, for these twenty amino acid residues.

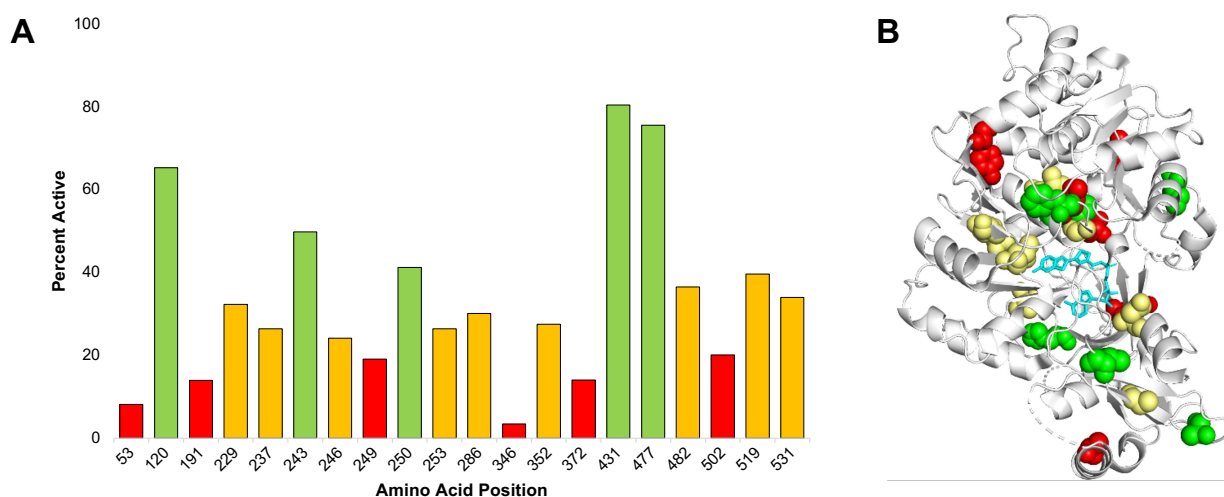


Figure 2. (A) Mutability of 20 SCA-identified amino acid positions as determined from a top-plating activity screen. Each library was transformed into bacteria and embedded in a thin layer of top agar containing IPTG and D-luc. After overnight incubation, dark- and bright-field images of each plate were captured, which were digitally superimposed. The number of total and light-emitting (active) colonies were counted, and the ratio of these values was taken to give the percent active proteins in each library. 200 total colonies were assessed per library. (B) SCA-identified positions were mapped onto the FLuc protein structure (PDB: 4G36, visualized with PyMol), where color corresponds to the mutability of that residue, and in cyan is shown the luciferyl adenylate intermediate analog 5'-O-[(N-dehydroluciferyl)-sulfamoyl]adenosine (DLSA).

Oftentimes, the mutability of amino acids is inferred from either natural sequence conservation patterns or the spatial position of the residues within the protein structure. Thus, we wondered if our data could be predicted by either of these biochemical parameters. Interestingly, there is little correlation between mutability as determined by the top-plating screen and natural variability among the 39 luciferase homologs used as inputs for SCA (**Figure S3**). For example, as one might expect, Y53 is 100% conserved across luciferase homologs and the Y53X library is only 8% mutable. On the other hand, A477 is 98% conserved in nature, yet less than a quarter of the mutations at that position inactivated the protein. We also compared the distance between the side-chain of each amino acid and the nearest atom on D-luciferin to mutability, once again finding no apparent correlation (**Figure S4**). These results reaffirm the complexity of the bioluminescence

mechanism, giving us confidence that our decision to screen saturation libraries was a suitably unbiased way to investigate this system. Collectively, we have generated a data set of the mutability of twenty amino acid residues that may facilitate engineering studies as well as the investigation of understudied regions of the protein; these positions demonstrate the utility of SCA as many of these sites would likely have not been identified using traditional approaches.

While the top-plating screen gives valuable information about the relative mutability of each position, it does not reveal which specific mutations inactivate the protein. To determine which specific mutations are inactivating, we used HT-Seq to count all mutants in both the active population and a pre-screen population. We considered mutations that are at least three-fold de-enriched in the active population relative to the pre-screen population to be likely inactivating mutations. By this measure, we found that 172 out of 380 library mutants (45%) are predicted to be inactive. We found that amino acid positions 53 and 346 were among the most de-enriched for activity, corroborating our finding from the activity screen that these two positions were the least mutable (8% and 3%, respectively). Y53 appears to favor mutations to other aromatic amino acids, implying a functional role for this aromatic side chain that is distant from the active site. T346 only tolerates mutation to cysteine, implying a need for hydrophobic character as well as a hydrogen bond donor in this amino acid that is near the substrate. On the other hand, the protein seems to tolerate a wide range of mutations at a number of positions such as N229, H431, and A477. Overall, these results enhance the utility of our activity screen on its own by revealing which specific amino acid sidechains, not simply which mutant positions, are more or less likely to impair catalysis. Although beyond the scope of this study, these data make for an exciting entry point to many novel biochemical hypotheses to further explore FLuc.

Identification of red-shifting mutations

This approach allowed us to take only the 208 active mutants forward to a secondary color screen. To assess emission wavelength, we used a previously reported screen which we have used to isolate mutants with red-shifted emission spectra in medium to high-throughput formats.²¹ Briefly, by comparing the filtered luminescence intensity at 620 nm (± 20 nm, 'red') and 528 nm (± 10 nm, 'green'), we can easily screen thousands of mutants for red-shifting while controlling for variations in protein expression and enzyme turnover; this ratio, or 'color score' has been previously shown to be an effective proxy for emission wavelength.²¹ We screened all active-enriched populations using this method.

As a first step to understanding emission color, we compared the color score of all mutants surveyed from each amino acid position (**Figure 3A**). By comparing the average color scores of all active members from each library, we can infer the general impact of mutations at specific amino acids on emission wavelength. While the wild-type enzyme consistently showed a mean color score of about 2.0, we found that libraries N229X (11.6), I237X (3.5), L286X (4.1), T352X (18.4), and H431X (6.6) displayed significantly increased mean color scores with respect to WT, implying many of the mutants at these positions possess red-shifted emission. These data are corroborated by the fact that prior studies have also found the mutations N229S/T, I237A, and H431Y to red-shift luminescence.^{5,24} On the other hand, L286 and T352 have not been shown to impact color previously. Further, 17 of the 20 libraries screened revealed higher median color scores than WT, which at once affirms the sensitivity of the luminophore to its protein environment and indicates that many mutations may lead to small red-shifts in FLuc emission. Notably, we find that the most red-shifting residues tightly clustered near the benzothiazole binding pocket on the FLuc tertiary structure (**Figure 3B**). In particular, the proximity of the side-chains from N229,

L286, and T352 to the 6' phenolate suggests that a wide range of point mutations at these positions may disrupt local stabilization of the oxyanion and lead to increased red emission (**Figure 3C**). Following screening, we collected all individual mutants possessing statistically significantly increased color scores relative to WT into a new red-shifted enriched population. For ease of analysis, we combined the mutants for groups of two or three amino acid positions together; we refer to these enriched populations from multiple amino acid positions as “pools”. Collectively, this approach has identified populations of likely novel mutations that alter the emission wavelength of FLuc towards the red region.

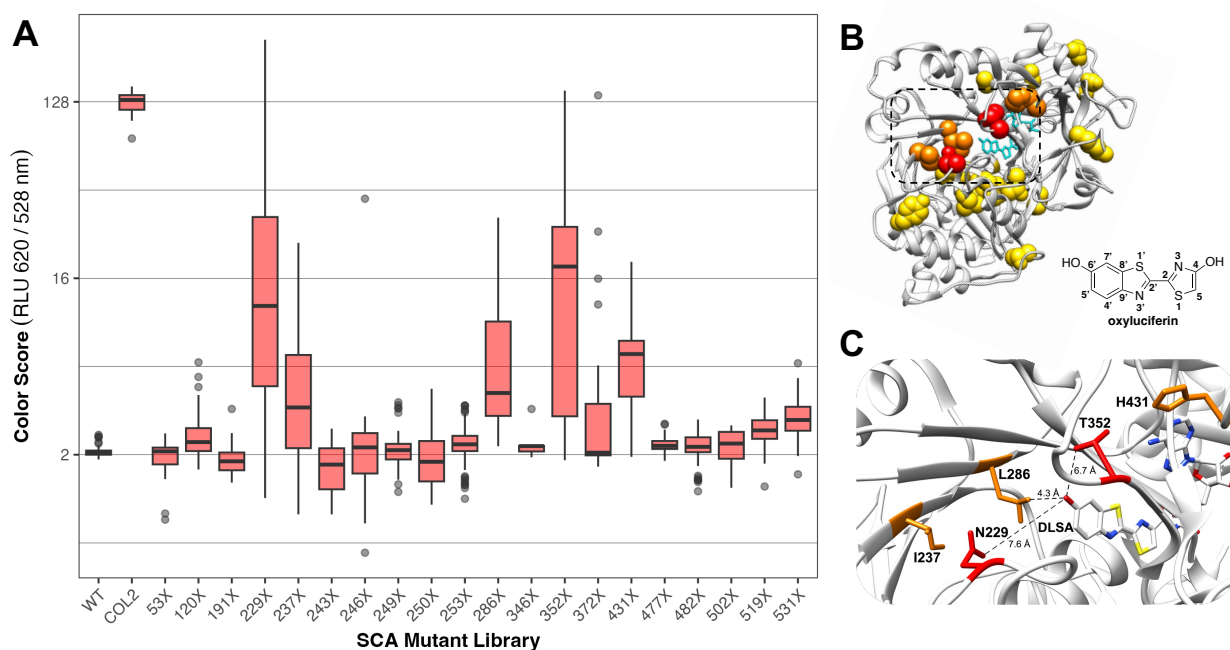


Figure 3. Color scores of each library from a screen for red-shifted mutants. **(A)** Active mutants were expressed in a 96-well format. The cells were lysed and combined with D-luc and ATP, then screened for luminescence using 620/40 nm and 528/20 nm optical filters. The ratio of these values is the color score, corresponding to red-shifted emission. Each plate contained WT FLuc and COL2 (a known red-shifted mutant) as internal controls; all experiments and controls are shown here. **(B)** The FLuc protein structure (PDB: 4G37, visualized with Chimera) is shown, with libraries displaying the five highest median color scores in red (N229, T352) and orange (I237, L286, H431), all other SCA-identified positions shown in gold, and DLSA (a luciferyl adenylate intermediate analog) shown in cyan. Also shown is the numbered phenol-enol form of oxyluciferin. **(C)** The boxed region in **B** is enlarged to illustrate the proximity of strongly red-shifting positions N229 and T352 (red) and moderately red-shifting positions I237, L286, and H431 (orange) to the 6'OH on DLSA (white, colored by heteroatom).

To validate that our screen effectively enriched the population for red-shifted mutants, we assayed the all active and red-shifted populations for color score (**Figure S5**). Gratifyingly, with the exception of pool 4, the red-shifted populations showed significantly higher color scores than the corresponding active populations ($p < 0.05$), indicating successful enrichment of red-shifted mutants (**Table S2**). These data demonstrate that our mutants reproducibly display a significant change in emission color.

Next, we sought to understand the specific mutations responsible for the red-shifted enzymes observed in the color screen. To do so, we used HT-Seq to compare the distribution of mutations in the active population relative to the red-shifted population. This allows us to calculate

an enrichment score for each mutant, which predicts which mutations cause a red-shift in the emission. Collectively, of the amino acid changes that are predicted to be active mutant proteins, 70 distinct amino acid changes are enriched in the red-shifted population (**Figure 4**). While mutations that red-shift emission are historically well-studied, an overwhelming majority of these mutations are novel and this work constitutes a large expansion in the total number of known red-shifting mutants.

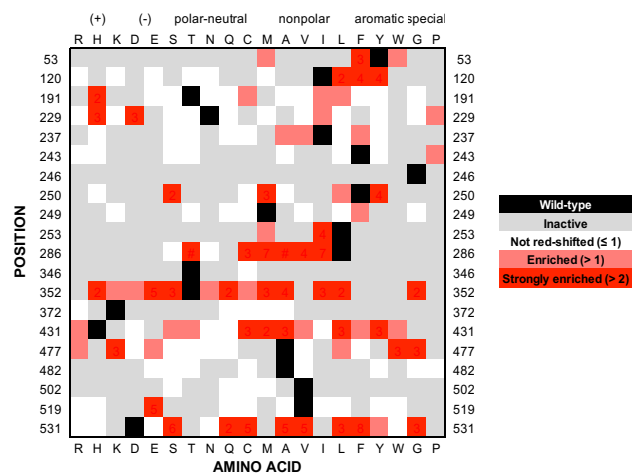


Figure 4. Sequence-function map of FLuc mutations at 20 SCA-identified positions. Mutants displaying visible bioluminescence in a top-plating screen were collected into an active population, and those displaying a color score at least two standard deviations above the WT mean were collected into a population enriched for red-shifted enzymes. The populations were quantified by HT-Seq. Mutants that were at least two-fold de-enriched in the active population with respect to the pre-screen population are shown in grey (“inactive”). Mutants predicted to be active are sorted by enrichment in the red-shifted population with respect to the active population, as white (de-enriched), pink (enriched), and red (at least two-fold enriched).

One advantage of our mutational scanning approach is that these data can also serve as a guide to which positions do not appear to red-shift FLuc emission regardless of the new amino acid; residues M249, T346, and A482 show strong de-enrichment in all cases for red-shifting. While it’s possible that other residues in those pools could have overshadowed any red-shifting mutations at these positions and led to the appearance of de-enrichment, these results nonetheless imply that universally de-enriched positions likely have minor effects on emission energy. In contrast to arguments that wholly attribute color to the polarity and openness of an exquisitely sensitive ‘microenvironment’ which, upon any perturbation, results in energy loss and red-shifting, these data suggest that some residues are irrelevant to this property and the phenomenon may not be quite so general. Thus, beyond identifying novel red-emitting luciferases, our broad and high-throughput approach allows us to localize color shifting effects to a concrete group of residues. Altogether, these results provide a novel set of red-shifting mutations that may expand our understanding of the complex mechanisms determining emission color.

Unsurprisingly, the amino acid positions that displayed high average color scores were also frequently broadly enriched in the red-shifted population. For example, T352, a position not previously known to impact emission color, showed enrichment when mutated to all 13 of the amino acids that were not inactivating, demonstrating that any mutation at this position appears to red-shift emission. These data imply that the threonine sidechain is likely taking part in some key interaction that, when disrupted, decreases the emission energy. L286 also reveals broad mutability with a large effect on emission wavelength, showing enrichment for mutation to 6 different amino acids, while H431 is enriched for 11 different amino acids and D531 for nine. On the other hand, some positions are enriched only for a subset of substitutions. Examples include Y53F/W, I120L/F, and I237V/A; at these positions, small steric alterations alone may suffice to red-shift emission in certain cases. Collectively, these data highlight a set of novel and important interactions at certain amino acid positions that red-shift the FLuc emission spectra.

Characterization of strongly red-shifted mutants reveals multiple emitters

While our workflow identifies mutations that significantly red-shift emission relative to FLuc WT, it does not reflect the magnitude of that change. To identify the mutants with the most red-shifted emission among the enriched population, we rescreened the red-shifted population for color and isolated and sequenced the five mutants with the highest color scores. The most red-shifted mutants showed strong sequence convergence, indicating that the recovered mutants did not emerge due to chance and rather lead to a reproducible effect on emission color by the mutation (**Table S3**). Importantly, all the mutations that showed convergence also showed enrichment in our high-throughput sequencing data. From among the isolated enzymes, mutations I120Y, G246S, F250S/Y, L286V/T, H431R, and D531G/A resulted in moderate color scores ranging from 2-12, while mutations T352M/Q and N229T/V/H gave color scores of 50 to well over 100, respectively, and possessed minimal green emission. Furthermore, the positions which displayed red-shifting enrichment for the greatest number of amino acids (L286, T352, H431, D531) were found to comprise all the recovered mutants from pools 4 through 7, affirming the success of the enrichment process. Thus, the sequence identity of these mutants strongly corroborates our prior population level HT-Seq data.

To confirm that these recovered mutants display authentically red-shifted emission, we collected full bioluminescence spectra of six red-shifted mutants from different pools: I120Y, N229T, L286V, T352M, H431R, and D531G (**Figure 5A**). Luciferase mutants were expressed in culture by autoinduction, lysed, and briefly incubated with ATP and D-luciferin, after which their full luminescence emission spectra were observed. Gratifyingly, the recovered mutants all display red-shifted emission spectra, indicating that the color scoring method successfully selected for red-shifted mutants during screening. To further quantify the red-shift, we calculated the portion of photons emitted above 600 nm in each bioluminescence spectrum, finding a clear correlation to the previously determined color score (**Figure S6**). Of the samples, the WT enzyme displays the

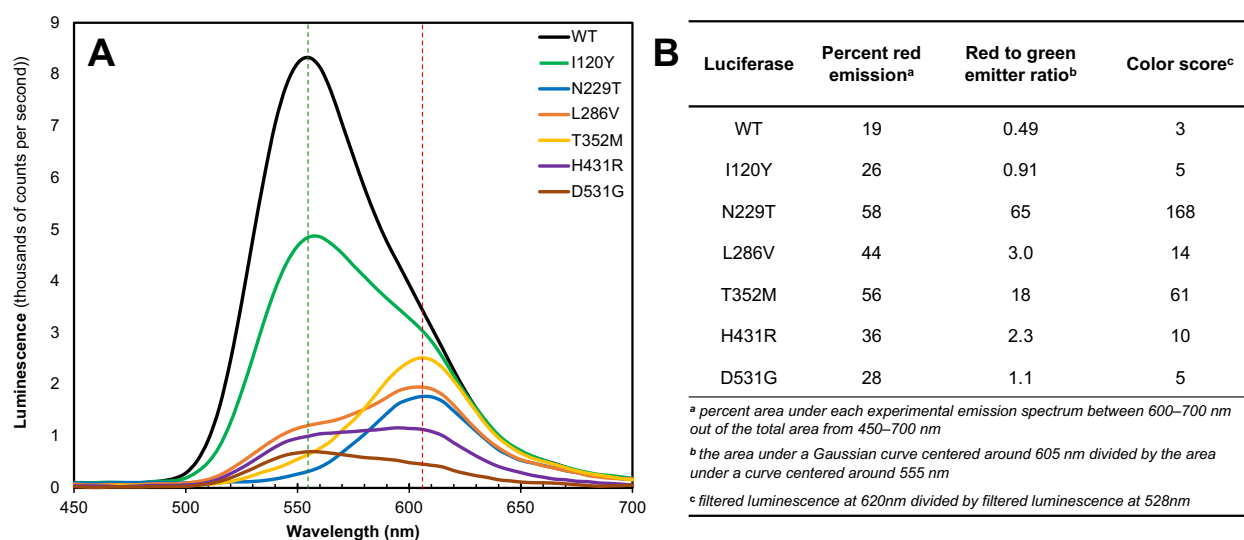


Figure 5. Bioluminescence emission spectra of red-shifted mutants. **(A)** Mutants displaying the highest color score from each red-enriched population were isolated and expressed. The cells were lysed and briefly incubated with D-luciferin and ATP, then the emission was recorded from 450–700 nm at room temperature and pH 7.5. **(B)** To quantify the red-shift displayed by each mutant enzyme, two Gaussian curves were fit to each spectrum corresponding to red (~605 nm, red dotted line) and green (~555 nm, green dotted line) oxyluciferin emitters. Color scores were determined in an independent screen of the recovered mutants (12 replicates per mutant).

lowest color score and the lowest percentage of red light emitted, while mutant N229T displayed the highest value by both heuristics (**Figure 5B**).

Interestingly, many of the mutants (I120Y, L286V, H431R, D531G) display emission spectra with two clear and distinct emission peaks, revealing one emitting species at approximately 555 nm (“green emitter”) and another at approximately 605 nm (“red emitter”). The other mutants (N229T, T352M) display pure unimodal emission corresponding to the red emitter only. This model agrees with recent arguments that attribute the differing luciferase emission wavelengths to combinations of multiple chemical states of oxyluciferin.^{7,25,26} Interestingly, we found that varying pH also affected the relative distribution of emitter states; the yellow-green emitter is highly destabilized under acidic conditions, while the λ_{max} of each emitter remained pH-insensitive (**Figure S7**). To quantify the relative contribution of each emitter to total luminescence, we modeled the normalized spectra as the sum of two Gaussians (**Figure S8, Table S4**), and compared the separate curves (**Table S5**). Mutations N229T and T352M appear to completely destabilize the green emitter, displaying 65- and 18-fold greater integrated luminescence from the red emitter, respectively (**Figure 5B**). In all cases, the amount of red light emitted by the enzymes corresponds to the relative abundance of the red- and green-emitting states rather than a significant shift in the λ_{max} , which appears to be delimited by unique emitters. Thus, the most red-shifting mutations which emerged from the color screen stabilize a distinct chemical form of oxyluciferin to varying degrees. The proportion of total luminescence in the red region can be enhanced by promoting this emitting species through mutagenesis.

DISCUSSION

In this work, we have rapidly identified a large number of novel red-shifting mutations in the *P. pyralis* luciferase. By comprehensively assessing twenty amino acid positions for red-shifting effects, we found that at least five of these residues display strongly red-shifted emission upon mutation to a variety of amino acids. Thus, N229, I237, L286, T352, and H431 can be easily targeted to yield luciferase mutants with emission peaking above 600 nm, and protein engineers may select from this variety at each position to maximize protein stability and other properties of interest. In addition to highlighting certain positions as important to emission color, we report 70 specific point mutations that are predicted to red-shift emission based on population-level HTSeq analysis. This expansion in the number of known red-emitting luciferases should prove a fruitful resource for the bioluminescence imaging community by providing an array of reporters with higher effective quantum yields *in vivo*; the greater percentage of red photons emitted will reduce the attenuation of light by tissue. While our focus has been on red-shifting FLuc emission, our high-throughput platform has also provided a set of active mutant enzymes that may readily be engineered further through screens for additional properties (e.g. thermostability, substrate selectivity, turnover). In addition to the applications of these findings to deep-tissue BLI and further engineering of the protein, they also provide a wealth of biochemical information about FLuc and how emission color is determined.

For instance, this large set of mutations with quantifiable effects on emission enables us to evaluate some recent hypotheses proposed about the color tuning mechanism among luciferases. While most of the saturation libraries we constructed displayed increased median color scores compared to the WT enzyme, implying broad and nonspecific red-shifting effects upon disruption of the active site environment, in most cases this effect was minor. Indeed, all but five or six of the libraries display median color scores that cluster near the WT score, demonstrating that few mutations at most sites red-shifted emission, and even those had modest effects (**Figure 3A**). This

observation suggests that the general ‘openness’ of the FLuc tertiary structure surrounding oxyluciferin, and the active site polarity more broadly, are not primarily responsible for emission color. Our results clearly bear out that not any amino acid mutation, or even the majority, will red-shift the emission simply by increasing energy loss from excited oxyluciferin to the environment. Rather, specific molecular interactions are at play, some of which emerge upon a closer look at the mutations that did have large effects on emission.

The bioluminescence emission spectra of red-shifted mutants recovered from color screening clearly indicate the presence of two distinct emitting species centered around 555 nm and 605 nm. It follows that the mechanism of color modulation by these mutations is alteration of the ratio of these two emitters, by preferential stabilization of one or the other. However, the specific interactions leading to this effect prove more elusive, as the mutations that significantly promote the red emitter (~605 nm) cluster on the tertiary structure around the benzothiazole ring of the substrate, in close proximity to the 6' hydroxyl (**Figure 3B**). This observation is initially surprising, as the most commonly proposed candidates for the red and green emitting oxyluciferin states are the keto and enol forms of oxyluciferin, yet tautomerization occurs on the opposite side of the substrate to the phenolate.^{14,24,25} That we observe such unambiguous clustering, in spite of the random spatial distribution of the positions we investigated, strongly suggests a meaningful local set of interactions. Had we set out to investigate a two-emitter hypothesis through deep mutational scanning of residues nearer to the site of tautomerization, we would have overlooked the functional importance of the benzothiazole binding pocket and related interactions. Indeed, we did not observe significant red-shifting from the libraries (e.g. G246, F250) that are nearest to the oxyluciferin thiazole ring. Clearly, more complex and delocalized interactions affect the ratio of emitting states—and it is precisely our impartiality with respect to any color tuning mechanism during library construction, deferring instead to SCA, that enabled us to reach this conclusion.

Specifically, these findings suggest a network of solvent-mediated interactions with the phenolate that may lead to alteration of the tautomeric ratio. The N229, L286, and T352 sidechains are all within 8 Å of the phenolate oxygen but are not within direct hydrogen-bonding distance (**Figure 3C**); while this distance makes direct contact unlikely, it's notable that the active site pocket near the phenolate is densely populated with up to six ordered solvent molecules in various crystal structures.²⁷ This implies a potentially crucial network of H-bonds formed between protein backbone or sidechain heteroatoms and coordinated waters that may stabilize the green emitter in WT FLuc. Notably, our data reveal that mutations to these three residues have broad red-shifting effects: at least five mutations at each position are enriched for red-shifting (**Figure 4**). The abundance of mutations near the 6' phenol strongly implies the loss of a key contact near the 6' oxygen that stabilizes the green emitter through cascading electronic effects on the C5 alpha proton—rather than the gain of a new interaction which stabilizes the red one, in which case we expect to see convergent enrichment for a single mutation. As deprotonation of the 6' phenol likely occurs in the excited state,^{8,28} it is possible that the native residues (N229, L286, and T352) facilitate deprotonation through the aforementioned water network, and disruption of these contacts may hinder proton transfer such that the excited keto-phenolate emitter decays, giving red emission, before tautomerization to the yellow-green enol form may occur. Conversely, we observe modest red-shifting effects from mutants I120Y, D531G, and H431R (**Figure 5A**), which can be explained by their structural position well outside of the benzothiazole binding pocket in the enzyme's oxidation conformation. In summary, our results suggest that mutations likely to red-shift emission function by disrupting a solvent network around the key 6' phenolate on oxyluciferin, thus stabilizing a defined red-emitting state of the molecule.

However, additional spectroscopic and computational experiments are needed to further explore this theory. In light of this work, and a recent model for color determination proposed by the Branchini group that similarly underlines the importance of a water network proximal to the phenolate,²⁹ we believe that modeling oxyluciferin interactions with this ordered water network would prove a fruitful approach for the theoretical chemistry and structural biology communities. We believe the large number of novel mutations identified here should provide a rich and useful data set for modeling the role of the protein in the color determination process. The fact that these mutations red-shift emission through solvent interactions in the binding pocket suggests that neither spectroscopic/solvent studies with free oxyluciferin, nor modeling of its direct contact with nearby residues, are representative of the true emissive behavior when complexed with FLuc. Further, our results demonstrate the stark challenges of a rational approach to identifying residues important to the complex problem of color determination. Rather, an unbiased search has quite organically highlighted a subset of key residues that cluster tightly around the benzothiazole water network, and the specific mutations we identified serve as a valuable starting point for the computational investigation of local perturbations that result in each case.

Collectively, these results strongly support the multiple-emitter hypothesis of color tuning, which assimilates aspects of the long-standing keto-enol mechanism and various ‘micro-environment’ hypotheses.^{8,25} This theory is especially compelling for its reconciliation of environmental protein-driven effects, which our mutational evidence demonstrate are clearly relevant, with our finding that the red-shifting effects of mutagenesis are discontinuous. Meanwhile, these findings conflict with earlier hypotheses such as the ‘open-closed’ model, which narrowly ascribes the emission wavelength to active site openness and thus freedom of movement of the substrate.³⁰ In this case, we would have observed a dispersed distribution of λ_{\max} among the red-shifted mutants in proportion to the molecular rigidity of bound oxyluciferin. Thus, the diverse array of red-shifting mutations revealed by our high-throughput biochemical approach can shed light on problems even as historically well-studied as bioluminescence color tuning. While we have assessed all the active proteins at each SCA-identified amino acid position for effects on emission wavelength, the mutability values determined for each WT residue could serve as a promising starting point to explore other biochemical questions about FLuc, from its pH sensitivity to substrate specificity. It is our hope that the catalog of novel red-shifting mutations we have identified here are incorporated by the protein engineering community alongside other established mutations to evolve luciferases that are at once redder, brighter, and more stable.

CONCLUSIONS AND LIMITATIONS

Here, we have employed screening to thoroughly assess twenty amino acid positions of firefly luciferase for their effects on emission color. By selecting residues predicted to be important for function broadly, we were able to identify a variety of novel, red-shifting mutations which display clear patterns in their emission characteristics and position in the protein structure. Through an unbiased search through a large number of mutations, this study both aids our biochemical understanding of the factors impacting the emission and enables ongoing efforts to develop improved biomolecular probes for *in vivo* imaging. Further work is needed to model and further elucidate the mechanistic basis of how these mutations stabilize the green and red emitting states via the local water network. Future work may help to confirm whether these mutations also cause red-shifting in homologous enzymes and recombine these and other mutations for biochemical insight.

MATERIALS AND METHODS

No unexpected or unusually high safety hazards were encountered.

Activity screen. 200 mutants per library were assessed for functional protein. Each library was transformed into chemically competent *Escherichia coli* BL21(DE3) cells (New England Biolabs). Following recovery, varying volumes of transformants were combined in culture tubes with 1 mL of a solution containing 20 $\mu\text{g mL}^{-1}$ kanamycin (Kan, Research Products International), 1 mM isopropyl β -d-1-thiogalactopyranoside (RPI), 200 μM D-luciferin (Gold Bio), and 1 mL of a solution containing 7 mg mL^{-1} agar (Acrōs Organics) and 40 mg mL^{-1} Luria Broth (LB, RPI), each prewarmed to 48 °C. The combined mixture was briefly mixed and immediately poured onto gridded square petri dishes (Fisher) containing LB-Kan agar (25 mL), then swirled to form an even layer and allowed to set prior to overnight incubation. Following 16–18 hours incubation at 37°C, each top-plated library was imaged in a dark room using an Andor i-Kon 936 charge-coupled device (CCD) camera that was pre-cooled to -70 °C and mounted on top of a custom dark box (Logemann Visualization Products). Following imaging (details in the supplemental methods), the number of light-emitting colonies was divided by the total number of colonies to determine the mutability of each library.

Color screen. Active mutants from each library were expressed as 500- μL autoinduction cultures³¹ in 96-well deep-well plates. Three WT FLuc, two COL2 samples (a positive control for red-shifting), and three blank cultures (no inoculate), were used as screening controls for each plate. Following 22–24 hours incubation at 25 °C and 225 rpm, the cells were pelleted by centrifugation and the supernatant removed. Each cell pellet was resuspended in 250 μL lysis buffer (75 mM Tris•HCl, 1.5% Triton-X, 3% glycerol, and 3 mg mL^{-1} lysozyme, pH 7.4). 25 μL of each lysate was transferred to individual wells of a white 96-well screening plate (Eppendorf) containing 50 μL 1.5 mM ATP and 225 μM D-luciferin in 100 mM sodium phosphate buffer (pH 7.8). The plate was immediately added to a Biotek H4 Synergy plate reader set to 37 °C and shaken for 30 s. The plate was incubated at 37 °C for 5 min and the luminescence was read with a 528/20 nm filter and 620/40 nm filter (1 mg mL^{-1} lysozyme, 150 μM D-luc, 1 mM ATP final concentration). The color score was determined for each mutant by dividing the luminescence at 620 nm by that at 528 nm; those displaying a color score at least two standard deviations above the WT average were classified as red-shifted.

Bioluminescence emission spectra. Red-shifted mutants recovered from the color screen were expressed as 1-mL autoinduction cultures in a 96-well deep-well plate. Following 24.5 hours incubation at 25 °C and 225 rpm, the cells were pelleted by centrifugation and the supernatant removed. Immediately before each assay, the cell pellets were resuspended in 1 mL lysis buffer (75 mM Tris•HCl, 1.5% Triton-X, 3% glycerol, 3 mg mL^{-1} lysozyme, pH 7.8) and transferred to a 1-cm quartz cuvette. To each lysate was added 1 mL 3 mM ATP and 1 mL 3 mM D-luc in 100 mM sodium phosphate (pH 7.8), and the mixture was incubated for 5 min (1 mg mL^{-1} lysozyme, 1 mM D-luc, 1 mM ATP final concentration). Bioluminescence spectra were recorded at room temperature using a FluoroLog-3 Spectrofluorometer (Horiba Scientific) operating without excitation. The emission was detected from 450–700 nm in 5 nm intervals with a slit width of 5 nm and 10 s integration. A blank spectrum was used to correct for baseline drift; this was similarly recorded by combining 1 mL lysis buffer with 1 mL each of D-luc and ATP.

SUPPLEMENTAL INFORMATION DESCRIPTION

Full experimental procedures and materials used, including oligonucleotide sequences and SCA computational details. Full luciferase sectors generated by SCA, curve fitting parameters, reproducibility of screens, comparison of mutability to conservation and substrate proximity, analysis and color scores of enriched populations, identity and additional emission characteristics of red-shifted mutants. Code for analyzing HT-Seq data is freely available here: <https://github.com/Leconte-Group/ColeeOberlagSimonetal2023>.

REFERENCES

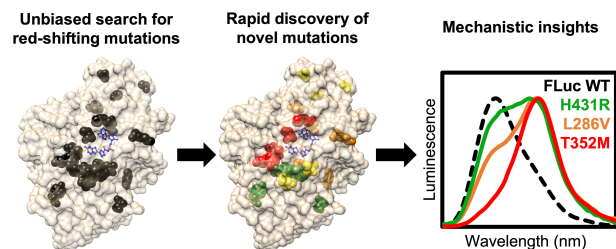
- (1) Davis, M. P.; Sparks, J. S.; Smith, W. L. Repeated and Widespread Evolution of Bioluminescence in Marine Fishes. *PLOS ONE* **2016**, *11* (6), e0155154. <https://doi.org/10.1371/journal.pone.0155154>.
- (2) Oba, Y.; Konishi, K.; Yano, D.; Shibata, H.; Kato, D.; Shirai, T. Resurrecting the Ancient Glow of the Fireflies. *Sci. Adv.* **2020**, *6* (49), eabc5705. <https://doi.org/10.1126/sciadv.abc5705>.
- (3) Zinn, K. R.; Chaudhuri, T. R.; Szafran, A. A.; O'Quinn, D.; Weaver, C.; Dugger, K.; Lamar, D.; Kesterson, R. A.; Wang, X.; Frank, S. J. Noninvasive Bioluminescence Imaging in Small Animals. *ILAR J. Natl. Res. Counc. Inst. Lab. Anim. Resour.* **2008**, *49* (1), 103–115.
- (4) Prescher, J. A.; Contag, C. H. Guided by the Light: Visualizing Biomolecular Processes in Living Animals with Bioluminescence. *Curr. Opin. Chem. Biol.* **2010**, *14* (1), 80–89. <https://doi.org/10.1016/j.cbpa.2009.11.001>.
- (5) Viviani, V. R. The Origin, Diversity, and Structure Function Relationships of Insect Luciferases. *Cell. Mol. Life Sci. CMLS* **2002**, *59* (11), 1833–1850. <https://doi.org/10.1007/PL00012509>.
- (6) Zhao, H.; Doyle, T. C.; Coquoz, O.; Kalish, F.; Rice, B. W.; Contag, C. H. Emission Spectra of Bioluminescent Reporters and Interaction with Mammalian Tissue Determine the Sensitivity of Detection in Vivo. *J. Biomed. Opt.* **2005**, *10* (4), 041210. <https://doi.org/10.1117/1.2032388>.
- (7) Carrasco-López, C.; Lui, N. M.; Schramm, S.; Naumov, P. The Elusive Relationship between Structure and Colour Emission in Beetle Luciferases. *Nat. Rev. Chem.* **2021**, *5* (1), 4–20. <https://doi.org/10.1038/s41570-020-00238-1>.
- (8) Al-Handawi, M. B.; Polavaram, S.; Kurlevskaya, A.; Commins, P.; Schramm, S.; Carrasco-López, C.; Lui, N. M.; Solntsev, K. M.; Laptinok, S. P.; Navizet, I.; Naumov, P. Spectrochemistry of Firefly Bioluminescence. *Chem. Rev.* **2022**, *122* (16), 13207–13234. <https://doi.org/10.1021/acs.chemrev.1c01047>.
- (9) Koksharov, M. I.; Ugarova, N. N. Strategy of Mutual Compensation of Green and Red Mutants of Firefly Luciferase Identifies a Mutation of the Highly Conservative Residue E457 with a Strong Red Shift of Bioluminescence. *Photochem. Photobiol. Sci.* **2013**, *12* (11), 2016–2027. <https://doi.org/10.1039/c3pp50242b>.
- (10) Naumov, P.; Ozawa, Y.; Ohkubo, K.; Fukuzumi, S. Structure and Spectroscopy of Oxyluciferin, the Light Emitter of the Firefly Bioluminescence. *J. Am. Chem. Soc.* **2009**, *131* (32), 11590–11605. <https://doi.org/10.1021/ja904309q>.
- (11) Branchini, B. R.; Southworth, T. L.; Khattak, N. F.; Michelini, E.; Roda, A. Red- and Green-Emitting Firefly Luciferase Mutants for Bioluminescent Reporter Applications. *Anal. Biochem.* **2005**, *345* (1), 140–148. <https://doi.org/10.1016/j.ab.2005.07.015>.

- (12) Carrasco-López, C.; Ferreira, J. C.; Lui, N. M.; Schramm, S.; Beraud-Pache, R.; Navizet, I.; Panjikar, S.; Naumov, P.; Rabeh, W. M. Beetle Luciferases with Naturally Red- and Blue-Shifted Emission. *Life Sci. Alliance* **2018**, *1* (4), e201800072. <https://doi.org/10.26508/lsa.201800072>.
- (13) Viviani, V. R.; Arnoldi, F. G. C.; Venkatesh, B.; Neto, A. J. S.; Ogawa, F. G. T.; Oehlmeier, A. T. L.; Ohmiya, Y. Active-Site Properties of Phrixotrix Railroad Worm Green and Red Bioluminescence-Eliciting Luciferases. *J. Biochem. (Tokyo)* **2006**, *140* (4), 467–474. <https://doi.org/10.1093/jb/mvj190>.
- (14) White, E. H.; Rapaport, E.; Seliger, H. H.; Hopkins, T. A. The Chemi- and Bioluminescence of Firefly Luciferin: An Efficient Chemical Production of Electronically Excited States. *Bioorganic Chem.* **1971**, *1* (1), 92–122. [https://doi.org/10.1016/0045-2068\(71\)90009-5](https://doi.org/10.1016/0045-2068(71)90009-5).
- (15) Branchini, B. R.; Ablamsky, D. M.; Rosenman, J. M.; Uzasci, L.; Southworth, T. L.; Zimmer, M. Synergistic Mutations Produce Blue-Shifted Bioluminescence in Firefly Luciferase. *Biochemistry* **2007**, *46* (48), 13847–13855. <https://doi.org/10.1021/bi7015052>.
- (16) Fowler, D. M.; Fields, S. Deep Mutational Scanning: A New Style of Protein Science. *Nat. Methods* **2014**, *11* (8), 801–807. <https://doi.org/10.1038/nmeth.3027>.
- (17) Starita, L. M.; Pruneda, J. N.; Lo, R. S.; Fowler, D. M.; Kim, H. J.; Hiatt, J. B.; Shendure, J.; Brzovic, P. S.; Fields, S.; Klevit, R. E. Activity-Enhancing Mutations in an E3 Ubiquitin Ligase Identified by High-Throughput Mutagenesis. *Proc. Natl. Acad. Sci.* **2013**, *110* (14), E1263–E1272. <https://doi.org/10.1073/pnas.1303309110>.
- (18) Halabi, N.; Rivoire, O.; Leibler, S.; Ranganathan, R. Protein Sectors: Evolutionary Units of Three-Dimensional Structure. *Cell* **2009**, *138* (4), 774–786. <https://doi.org/10.1016/j.cell.2009.07.038>.
- (19) Socolich, M.; Lockless, S. W.; Russ, W. P.; Lee, H.; Gardner, K. H.; Ranganathan, R. Evolutionary Information for Specifying a Protein Fold. *Nature* **2005**, *437* (7058), 512–518. <https://doi.org/10.1038/nature03991>.
- (20) McLaughlin Jr, R. N.; Poelwijk, F. J.; Raman, A.; Gosal, W. S.; Ranganathan, R. The Spatial Architecture of Protein Function and Adaptation. *Nature* **2012**, *491* (7422), 138–142. <https://doi.org/10.1038/nature11500>.
- (21) Liu, M. D.; Warner, E. A.; Morrissey, C. E.; Fick, C. W.; Wu, T. S.; Ornelas, M. Y.; Ochoa, G. V.; Zhang, B.; Rathbun, C. M.; Porterfield, W. B.; Prescher, J. A.; Leconte, A. M. Statistical Coupling Analysis-Guided Library Design for Discovery of Mutant Luciferases. *Biochemistry* **2018**, *57* (5), 663. <https://doi.org/10.1021/acs.biochem.7b01014>.
- (22) Blanco, C.; Verbanic, S.; Seelig, B.; Chen, I. A. EasyDIVER: A Pipeline for Assembling and Counting High-Throughput Sequencing Data from In Vitro Evolution of Nucleic Acids or Peptides. *J. Mol. Evol.* **2020**, *88* (6), 477–481. <https://doi.org/10.1007/s00239-020-09954-0>.
- (23) Sotomayor-Vivas, C.; Hernández-Lemus, E.; Dorantes-Gilardi, R. Linking Protein Structural and Functional Change to Mutation Using Amino Acid Networks. *PLoS ONE* **2022**, *17* (1), e0261829. <https://doi.org/10.1371/journal.pone.0261829>.
- (24) Ugarova, N. N.; Maloshenok, L. G.; Uporov, I. V.; Koksharov, M. I. Bioluminescence Spectra of Native and Mutant Firefly Luciferases as a Function of pH. *Biochem. Mosc.* **2005**, *70* (11), 1262–1267. <https://doi.org/10.1007/s10541-005-0257-2>.

- (25) Wang, Y.; Akiyama, H.; Terakado, K.; Nakatsu, T. Impact of Site-Directed Mutant Luciferase on Quantitative Green and Orange/Red Emission Intensities in Firefly Bioluminescence. *Sci. Rep.* **2013**, *3* (1), 2490. <https://doi.org/10.1038/srep02490>.
- (26) Hirano, T.; Hasumi, Y.; Ohtsuka, K.; Maki, S.; Niwa, H.; Yamaji, M.; Hashizume, D. Spectroscopic Studies of the Light-Color Modulation Mechanism of Firefly (Beetle) Bioluminescence. *J. Am. Chem. Soc.* **2009**, *131* (6), 2385–2396. <https://doi.org/10.1021/ja808836b>.
- (27) Branchini, B. R.; Fontaine, D. M.; Southworth, T. L.; Huta, B. P.; Racela, A.; Patel, K. D.; Gulick, A. M. Mutagenesis and Structural Studies Reveal the Basis for the Activity and Stability Properties That Distinguish the Photinus Luciferases Scintillans and Pyralis. *Biochemistry* **2019**, *58* (42), 4293–4303. <https://doi.org/10.1021/acs.biochem.9b00719>.
- (28) Falklöf, O.; Durbeej, B. Distinguishing between Keto–Enol and Acid–Base Forms of Firefly Oxyluciferin through Calculation of Excited-State Equilibrium Constants. *J. Comput. Chem.* **2014**, *35* (30), 2184–2194. <https://doi.org/10.1002/jcc.23735>.
- (29) Branchini, B. R.; Southworth, T. L.; Fontaine, D. M.; Murtiashaw, M. H.; McGurk, A.; Talukder, M. H.; Qureshi, R.; Yetil, D.; Sundlov, J. A.; Gulick, A. M. Cloning of the Orange Light-Producing Luciferase from Photinus Scintillans—A New Proposal on How Bioluminescence Color Is Determined. *Photochem. Photobiol.* **2017**, *93* (2), 479–485. <https://doi.org/10.1111/php.12671>.
- (30) Nakatsu, T.; Ichiyama, S.; Hiratake, J.; Saldanha, A.; Kobashi, N.; Sakata, K.; Kato, H. Structural Basis for the Spectral Difference in Luciferase Bioluminescence. *Nature* **2006**, *440* (7082), 372–376. <https://doi.org/10.1038/nature04542>.
- (31) Studier, F. W. Protein Production by Auto-Induction in High Density Shaking Cultures. *Protein Expr. Purif.* **2005**, *41* (1), 207–234. <https://doi.org/10.1016/j.pep.2005.01.016>.

FOR TABLE OF CONTENTS ONLY

TOC Graphic



Synopsis

We report dozens of novel amino acid mutations that red-shift Firefly Luciferase emission. The most red-shifting mutations reveal mechanistic insights about the basis of emission color and improve the enzyme's sensitivity in bioluminescence imaging.